

Keywords: automotive brake tester; roller; optimisation; PSI-method; finite element analysis; R1MS

Yulian ANGELOV, Ivo DRAGANOV*

University of Ruse

8 Studentska str., 7017, Ruse, Bulgaria

*Corresponding author. E-mail: iivanov@uni-ruse.bg

SOME GUIDANCE IN THE DESIGNING OF A ROLLER FOR THE AUTOMOTIVE TESTERS

Summary. This work presents some aspects related to the designing of a roller for stands that are intended to determine the parameters of the transmission of a vehicle, such as braking force, wheel revolutions, etc. The computational scheme of simply supported beam is used to create an analytical mechanical-mathematical model through which a multicriteria optimization problem has been solved. A finite element macro and submodel of the roller has been created, and by using the R1MS technique, the fatigue strength in the welding seams in the roller has also been determined. A parametric analysis is accomplished to determine the influence of the thickness of the base steel and the covering ebonite layer on the perimeter change of the outer surface, taking into account the physical non-linearity of the outer layer.

1. INTRODUCTION

There are currently a number of directives and standards in the European Union requiring periodic checks on both the suspension of motor vehicles [1], [2], and [3] and the systems associated with it [4] and [5]. For this purpose, stands with different designs are constructed which, depending on the principle of action, can be classified as dynamic, kinematic, and static. The most widely used applications are the rollers [6], [7]. They are applied to the diagnosis of motorcycles, light and commercial vehicles weighing up to 3.5 tonnes, with a brake force range of up to 10 kN, and for trucks with a brake force range of up to 40 kN. The braking forces are determined separately for each wheel on one axis of the vehicle. For this purpose, it is used the torque applied to the roller of the wheel drive when the brakes are applied. A scheme of such a stand is given in Fig. 1.

The importance of the braking system is based on the study of the influence of various parameters on the work process of the roller stands, such as tire pressures [8] and [9], standout system [10] and [11] and braking disc condition [12]. Regardless of its relatively simple construction, it should be indicated that the rollers are the working elements of the stands that come into direct contact with the tire and the conditions that they have to meet are various and contradictory. This raises a number of questions concerning their design, which must be considered in the light of current design trends [13].

The stand roller is subjected to a force caused by its contact with the wheel of the vehicle on one hand and the connection in the bearing supports on the other. This allows the roller to be regarded as a simply supported beam and be solved by using the analytical methods of mechanics [14] and [15]. This model is suitable when it is necessary to optimize the main dimensions of the roller, especially if there are more than one criterion [16], [17]. Another possibility of analyzing the stressed and strained state, allowing the indication of more complex geometric shapes, is to use the finite element method [18].

The operating conditions associated with cyclic loads require the problem for the existence of fatigue strength of the rollers to be considered. As it is a welded structure, it is extremely important to

indicate the stresses in the welding seams and their surrounding area. A widespread method to calculate the fatigue, using the finite element method, is Radius 1 millimeter–Mean Scatter (R1MS), proposed by Radaj [19]. Because of the large volume of computational work, the application of this technique involves the creation of sub-models [20].

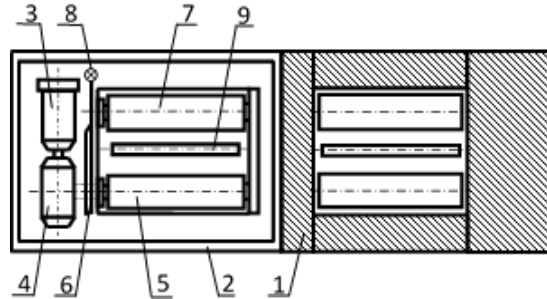


Fig. 1. A scheme of a roller testing machine: 1-right part; 2-left part; 3-electric motor; 4-gear reducer; 5-drive roller; 6-spoke gear; 7-calibration roller; 8-dynamometer; and 9- lock roller [6]

The non-slip requirement between the stand roller and the tire of the vehicle determines the use of an additional layer of high friction coefficient. Often, for the coating of the steel core, an ebonite which has non-linear material characteristics as described by Davie [21] is used.

The question of delamination of the layers studied by a number of authors [22] and [23] is beyond the scope of the present study, assuming the necessary cohesiveness in the process of vulcanization of the ebonite.

2. SOLVING AN OPTIMIZATION PROBLEM TO DETERMINE THE MAIN SIZES OF THE ROLLER

2.1. Mechanical-mathematical model

The mechanical-mathematical model is established for the case of maximum braking effort of the vehicle. This occurs at the moment when the process of interaction passes from a non-slip condition to a relative slippage of the contact surfaces of the tire and the roller, whereby the stand system must stop the torque. Under these conditions, the stand and the vehicle are presented as the holonomic mechanical system shown in Fig. 2.

The contact area between the tire and the roller represents a one-sided joint defined by the direction of normal force N and the frictional force T . Indicating the equilibrium of the mechanical system, it is possible for the forces of interaction between the rollers of the stand and the tire of the vehicle to be found. The normal force and the frictional force are calculated according to the equation:

$$N = \frac{G(r_r + r_a)}{\sqrt{4(r_r + r_a)^2 - e_r^2}}, \quad T \leq \mu_0 N, \quad (1)$$

where G is half the weight of the axis of the measured vehicle, μ_0 is the coefficient of friction for slipping, and r_r , r_a , and e_r are geometric parameters taken from the calculation diagram of the stand represented in Fig. 2.

In the process of measuring the braking efficiency, the frictional force T is of varying magnitude, resulting in a change of the magnitude and direction of its (counter) equating force

$$F = \sqrt{N^2 + T^2}, \quad \alpha = \text{atctan}(T/N). \quad (2)$$

The precondition for a concentric load in the middle of the roller's length is acceptable as this does not result in a significant change in the mechanical condition being studied. Because of the symmetry in the transverse direction of the roller and in neglecting its own weight, the calculated scheme is represented as a simply supported beam (Fig. 3).

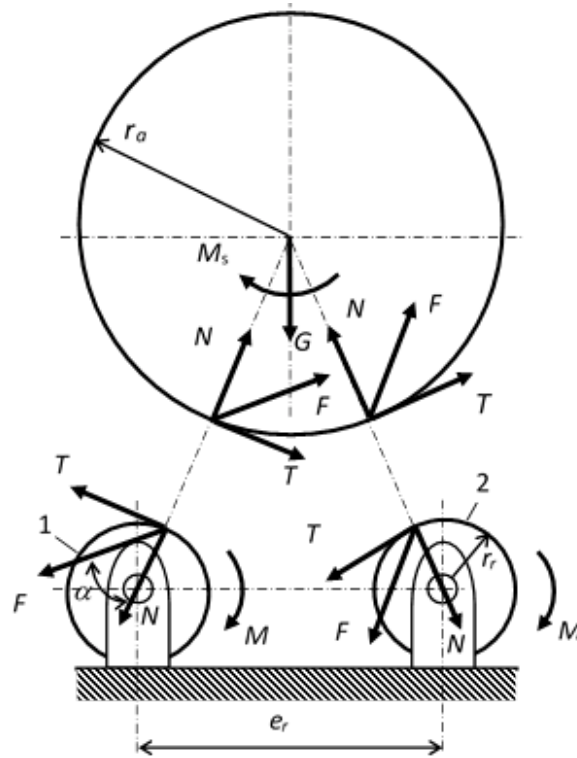


Fig. 2. Computational scheme of a roller stand for measuring the braking efficiency

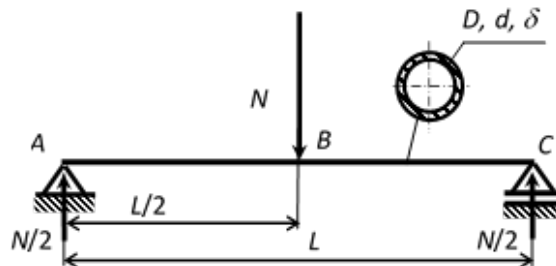


Fig. 3. Computational scheme of the roller

By neglecting the tangential tensions by twisting and pure slipping, the roller is subjected to bending. Under these conditions, the maximum normal stress in the load plane is obtained:

$$p_{max} = 8NL / [\pi D^3 (1 - d^4 / D^4)] \tag{3}$$

where D , d and L are, respectively, the outer and inner diameters and the length of the roller.

The equation of the elastic line is used to obtain the maximum displacement of the roller in the plane of the load:

$$w_{max} = 4NL^3 / 3\pi ED^4 (1 - d^4 / D^4), \tag{4}$$

where E is the Young's modulus.

Another feature, a study's object, is the mass of the roller for which it is used in the following relationship:

$$m_r = \pi\rho L(D^2 - d^2) / 4, \tag{5}$$

where ρ is the density of the roller's material.

2.2. Research concerning the model and analysis of the found results

In conducting numerical experiments, the quantities (3), (4), and (5) are brought into non-dimensional form by referring to their values for the prototype:

$$p = p_{\max} / p_{\max,p}, \quad w = w_{\max} / w_{\max,p}, \quad m = m_r / m_{r,p}. \quad (6)$$

Varying parameters of this study are the dimensions of the cross-section of the roller D , d , and δ , where between them, the analytical relationship $D = d + 2\delta$ is valid.

Equations (3), (4), and (5) are non-linear functions of the second, third, and fourth degree of the varying parameters. To clarify the influence of these parameters, two studies with additional restrictions have been accomplished. For this purpose, some relevant computer programs are established and numerical experiments are done in the specialized programming environment MATLAB [24].

The study of the change concerning the maximum stresses p and maximum displacements w of the braking stand's rollers for the roller's outer diameter of the braking stand is set to be conducted in the range of $0.14 \leq D \leq 0.24$, measured in meters. For the outer diameter of the roller and the condition of a constant mass of the prototype's rollers, leads to the results in the limit of $d = (D^2 - 0.0044)^{1/2}$. The values of the modifiable parameters of the model are $L = 0.8$ m; $\rho = 7850$ kg/m³, $E = 200$ GPa, $G = 17.168$ kN, $r_c = 0.4$ m, and $e_r = 0.45$ m.

The results of numerical experiments are graphically presented in Fig. 4. The change in the maximum non-dimensional stresses is marked by 1 and the maximum non-dimensional displacements is marked by 2. The relationships 1 and 2 are similar, show the same tendency of variation in the investigated interval, and differently satisfy the strength and strain conditions. For $D = 0.18$ m is equal to 1 in Fig 4 and correspond to the prototype's normalized dimensions: $p_{\max,p} = 14$ MPa and $w_{\max,p} = 0,041$ mm, and the mass of the roller is $m_{r,p} = 20.6$ kg. The maximum frictional force is $T_{\max} = 9.66$ kN and the load on the roller is $F = 13.66$ kN.

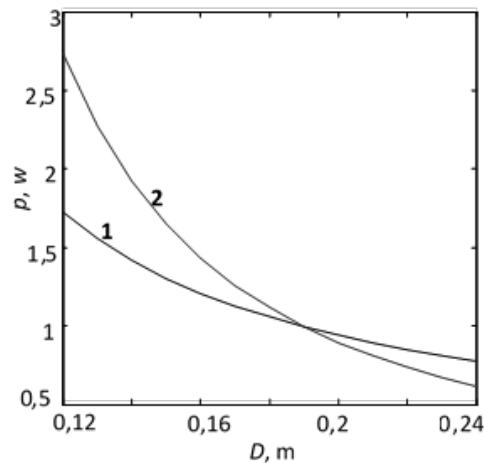


Fig. 4. Change of the relative maximum stresses 1 and maximum displacements 2

The investigation of the change of the maximum non-dimensional stresses and the relative mass of the rollers of the braking stand (Fig. 5) is set to be in the range of $0.11 \text{ m} \leq d \leq 0.18 \text{ m}$ for the internal diameter of the roll where there is no limit to its wall thickness. For non-variation of the braking system gauges, the outside diameter $D = 0.18$ m of the prototype is assumed to be constant. The analysis of the results shows that there is a conflict in these relationships, which is a prerequisite for seeking an optimal solution.

2.3. Parametric optimization

The optimization task is fulfilled by carrying out numerical experiments based on a simulation model containing a parametrically controlled mathematical model of the investigated object, a defined range of the parameters in which the solution is sought, and the space of the criteria of quality for which the extreme values are sought.

For this aim, the equations from (1) to (6) are used. The sizes of the cross-section of the roller, D , d , and δ , are selected to be the control parameters \mathbf{u} of the model, as based on the analytical relation $D = d + 2\delta$; it is determined that the internal diameter d has to be the estimating parameter.

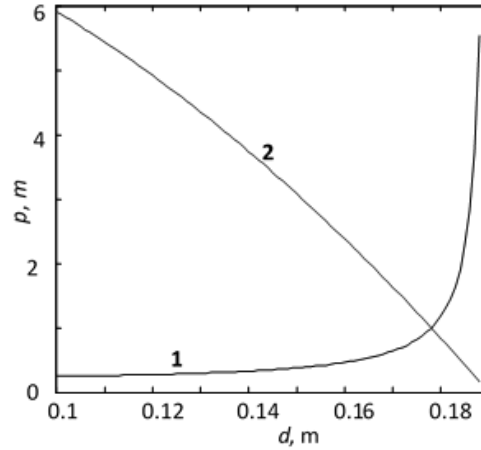


Fig. 5. Change of relative maximum displacements 2 and mass 1

All the other parameters G , L , ρ , E , and μ_0 are used to form the non-controlled parameter vector $\mathbf{q} \in \mathbf{Q}$.

Within the range of the optimization problem, the maximum normal stresses are transformed into a restriction representing an inequality:

$$p_{\max}(\mathbf{u}, \mathbf{q}) \leq p_{Lim}, \quad (7)$$

where p_{Lim} is the limit value of the normal stress.

After the implementation of the interval limits $[\mathbf{u}^-, \mathbf{u}^+]$ for the elements of the parameter vector \mathbf{u} is accomplished, the mathematical model can be summarized and presented in the following way:

$$\Psi(\mathbf{u}, \mathbf{q}) = 0, \quad \mathbf{u} \in \mathbf{U} := \{\mathbf{u} \in \mathbf{E}^3 : \mathbf{u}^- \leq \mathbf{u}^+\}, \quad \mathbf{q} \in \mathbf{Q}. \quad (8)$$

It is assumed that to evaluate the quality of the stand's rollers, the dimensionless values of the prototype, in terms of the characteristics $w_{\max,p}$ and $m_{r,p}$ of the relative maximum displacement and the relative mass, are used:

$$\phi_1 \equiv m = m_r / m_{r,p}, \quad (9)$$

$$\phi_2 \equiv w = w_{\max} / w_{\max,p}. \quad (10)$$

By using the equations (9) and (10), the vector criterion for assessing the quality of the investigated object is summarized in the following way:

$$\Phi(\mathbf{u}) \in \mathbf{K} := \{\phi_1, \phi_2\}. \quad (11)$$

Equations (8) and (11) are used to define the vector optimization problem:

$$\mathbf{u}^0 = \text{opt}_{\mathbf{u}}\{\Phi(\mathbf{u})\}, \quad \Phi(\mathbf{u}) \in \mathbf{K}, \quad \mathbf{u} \in \mathbf{U}, \quad \mathbf{q} \in \mathbf{Q}, \quad \Phi(\mathbf{u}) \in \mathbf{K} \quad (12)$$

where "opt" is an operator to simultaneously minimize the private criteria $\Phi(\mathbf{u})$, according to the principle of V. Pareto.

The solution of equation (12) represents the finding of such an acceptable control vector $\mathbf{u}^0 \in \mathbf{U}$, which minimizes the vector criterion (11) in the abovementioned sense. In the criterion range, this solution represents a plurality of Pareto-optimal points that are incomparable with each other. Choosing a compromise solution requires scaling the criterion (11) with a selected compromise scheme.

The possibility of equally approximating the private criteria to their ideal values is accomplished by the compromise scheme proposed in [16], which is based on the concept of a "utopian" point ϕ^* belonging to the criterion range. For the criterion defined in (11), range of \mathbf{K} , the generalized criterion, can be given in the following way:

$$\phi^S(\mathbf{u}) = \sum_{v=1}^k w_v (\phi_v^0(\mathbf{u}) - \phi^*)^2, \quad k = 2, \quad w_v = 1/2. \quad (13)$$

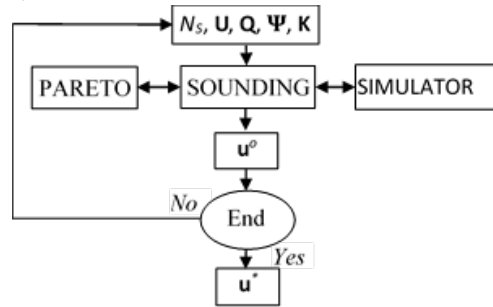


Fig. 6. Scheme of the computing process

To solve the optimization problem (12), a computational technology [17], based on a quasi-uniform sounding of multidimensional parametric areas on the PSI method (Parametric Space Investigation), and the selection of a set of approximately favorable solutions satisfying the Pareto-optimization principle, according to the diagram in Fig. 6 of the computation process, are used.

The multicriteria optimization problem is performed in accordance with $N_s = 4096$ Sobolev sample points belonging to the defined parameter area \mathbf{U} .

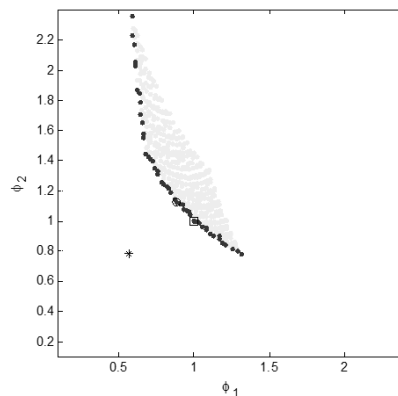


Fig. 7. Achievable set \mathbf{K} : utopia point (*), compromise solution (o), and a solution of the prototype (□)

The achievable set of the solution in \mathbf{K} is represented in Fig. 7. It defines a plurality of 166 Pareto-optimal points, depicted in the figure in black color. The utopic current point ϕ^* corresponding to the uncompromising minima of the vector criterion, used for evaluating the quality of the stand's roller (13), has the values shown in the brackets ($\phi^*_1 = 0.5977$; $\phi^*_2 = 0,7805$) and is depicted in Fig. 7, where the symbol (*) is used.

According to the criterion summarized in (12), optimal solution is determined [\mathbf{u}^s , $\phi^s(\mathbf{u}^s) = 0.441$], where the levels of the compromise of the private criteria, respectively, are $\phi^*_1 = 0.92252$ and $\phi^*_2 = 1.07887$, as it is shown in Fig. 7 by using the symbol (o), are found. The corresponding values of the controlled vector \mathbf{u}^s are given in meters $D = 0.17995$ m, $d = 0.16891$ m, and $\delta = 0.00552$ m.

In Fig. 7, the symbol (□) is used to represent the solution of the achievable set of the prototype's parameters of the investigated object at $D = 0.18$ m; $d = 0.168$ m, and $\delta = 0.006$ m. It also belongs to the Pareto plurality, but it is a prioritized criterion for minimizing the maximum relative displacements. The optimal solution found under criterion (13) provides a better balance between the private criteria by satisfying the principle of their equivalence.

3. SOLVING THE PROBLEM OF THE WELD'S FATIGUE STRENGTH

3.1. Geometric pattern

The roller is a rotationally symmetrical detail—Fig. 8, having symmetry in the longitudinal direction. The steel part that comes into contact with the wheel of the vehicle is covered with an ebonite layer for better grip.

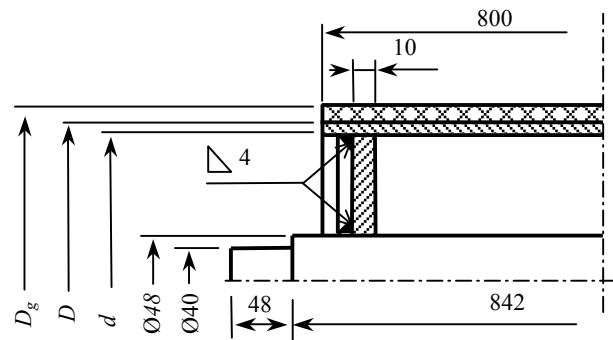


Fig. 8. The geometry of the roller (D_g — external diameter of the roller, D —diameter between ebonite, and steel, d — inner diameter of the roller)

3.2. Finite element model

To investigate the stress and strain state of the roller, the program system ABAQUS is used [25]. A simplified geometric model is established—Fig. 9a without taking into account the ebonite layer. An area for setting the load on the wheel of the car with a total contact area of 0.0176 m^2 is defined, which corresponds with the experimentally determined range described in [26]. Because of the symmetry, one-fourth of the roller is modeled.

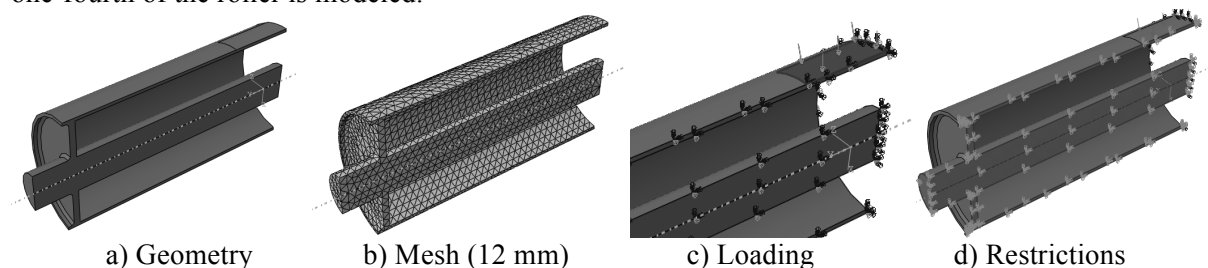


Fig. 9. Finite element model of the roller

The macro model of the roller is discretized with tetrahedral finite elements having intermediate nodes—Fig. 9b. Three densities of mesh are used. The load is set as a distributed load with an equivalent force $N/4$ —Fig. 9c. Fastening is realized by restricting all the degrees of freedom of the end of the shaft, and the symmetry is set on the transverse and longitudinal planes—Fig. 9d.

The material used in the manufacturing of the roller's details is set to be steel S235 with ultimate strength $\sigma_B = 360 \text{ MPa}$. The Poisson's ratio is set to be 0.27.

The results found after the macro model analysis are used to create a submodel of the welding seams, cutting out the zone with the largest tension stresses. This zone is critical for the strength and it is possible to occur rupture. The radii of curvature in transition from the seam to the detail is set to be with a magnitude of 1. The boundary conditions of the macro model are initially defined. The discretization of the model has also been performed with tetrahedral elements having one intermediate node.

The determination of the fatigue strength is accomplished in accordance to the relation proposed in [27], associated with the ultimate strength when the detail is under static load: $\sigma_{-1} = 0.32\sigma_B = 115.2$ MPa.

3.3. Results and analysis

The results for the macro model are given in Table 1. A diagram of the distribution of the first principal stress in the roller macro model is given in Fig 10a.

Table 1
Results of the analysis for macro model by using FEM

Solution No	Size of the elements, mm	Number of nodes	Total displacement, mm	Maximum von Mises stress in roller, MPa	Maximum first principal stress in welding seam, MPa
1	12	16626	0.608	147	10
2	6	79165	0.603	148	16.5
3	3	505709	0.611	148	35

As it can be expected, the maximum stresses appear in the middle, which coincides with the load area. The weld seams are located at a distance from the zones, where the boundary conditions are applied, and this implies the validity of the Saint-Venant principle. Due to edges with a zero radius of curvature in the welding seams, the results are not convergent, as can be seen in the last column of Table 1.

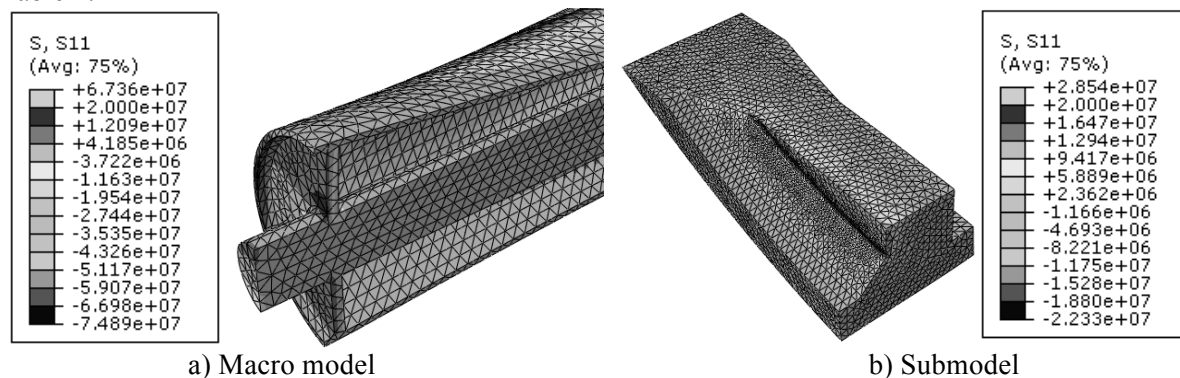


Fig. 10. First principal stress

The results found for the submodel are given in Table 2. Figure. 10b represents a diagram of the distribution of the first principal stress in the submodel. The maximum-obtained first principal stress is 30.5 MPa and, as it can be seen from the last column of Table 2, the result is convergent. The resulting first principal stress is less than the fatigue strength.

Table 2
Results of the analysis of the submodel

Solution No	Size of the elements, mm	Size of the elements in the compression zone, mm	Number of nodes	Maximum first principal stress in welding seam, MPa
1	1	0.4	89907	28.9
2	1	0.2	128536	30.5
3	1	0.1	238712	29.7

4. INVESTIGATION OF THE INFLUENCE OF THICKNESS OF THE EBONITE LAYER ON THE ACCURACY OF THE CALIBRATION ROLLER

4.1. Geometric model and material properties

The need to solve contact problem requires the construction of a geometric model of the roller and a part of the auto's tire.

The remaining sizes of the roller, the diameter between the ebonite and steel layers, and the inner diameter of the steel layer (Fig. 8) are selected according to chapters 2 and 3.

As the research object is the roller, the geometric model of the tire was built simplified in order to minimize the computational time of the task. The more significant assumptions are as follows: it is assumed that the contact surface between the tire and the roller is a plane, where the tire tread depth is not taken into account and the thickness of the tire is considerably larger than the existing one-chamber tires. It is assumed that a significant impact on the results will have a width of the tire, assuming that its value is 155 mm, with a radius of curvature of 20 mm. Because of the symmetry, just a quarter of the tire is investigated.

It is assumed that the steel part of the roller and tire will only operate within the elastic range and the relationship between the stresses and strains will be linear. The Young's modulus for the tire is 0.01 GPa and the Poisson's ratio is 0.45. Ebonite is a material with a non-linear relation between the stresses and strains and since it is expected that the deformations in it will have the most significant influence on the studied parameters, the problem has to be solved defining it as physically non-linear, where the information for the material characteristics is given in Table 3. It is assumed that its Poisson's ratio is 0.39.

Table 3

Material non-linearity of ebonite

Point	Stress, MPa	Strain, [-]
1	3	0
2	4	0.33
3	10	5

4.2. Discretization, boundary conditions, and contact

The roller is fixed by restricting all the degrees of freedom of the shaft's end, and the planes of symmetry are also defined. The tire is fixed by limiting the planes of symmetry and the degrees of freedom in the plane in normal direction for the outer surface of the tire.

The tire has a distributed load in the transverse direction with an intensity of 0.3781 MPa, which is equivalent to the assumed concentrated force N .

The discretization of the roller and tire has been performed by using hexahedral finite elements having one intermediate node (C3D20R) [25]. A check of the convergence is accomplished, comparing the results of the change of the roller's outer diameter for two mesh densities—13996 and 83596 nodes. The difference in results is less than 2%.

The strain state of the roller is determined by solving a contact problem for the interaction between the calibration roller and tire, without taking friction into account.

For the better computational algorithm operation, the tire is chosen to be discretized with elements that are larger than the ones of the roller [25].

4.3. Results and parametrical analysis

Radial movement of the outer contours of the middle one and another six sections, displaced in the axial direction through 10 mm, is indicated - Fig. 11.

The definition of the contour's perimeter– P' for the deformed roller, based on the values obtained for the displacement, can be accomplished by using the following equation:

$$P' = \sum_{i=1}^n u_{ri} \pi / n, \tag{13}$$

where u_r is the displacement in the radial direction and n is the number of points in the circular direction for which the displacement is determined.

Table 4 shows the sectional variations at $D_g = 196$ mm and $D = 180$ mm, defined as the difference between the initial perimeter, which is $P' = 615.75$ mm, and the perimeter of the deformed roller.

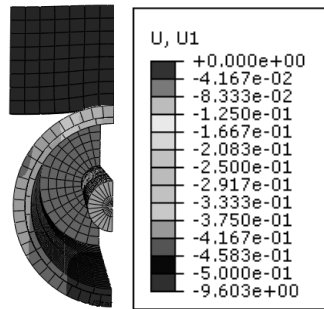


Fig. 11. Displacement in radial direction

The finite element model is used to study the influence of the thickness of the ebonite and steel layers on the variation of the outer perimeter of the roller's median section. The results of the parametric analysis are given in Fig. 12.

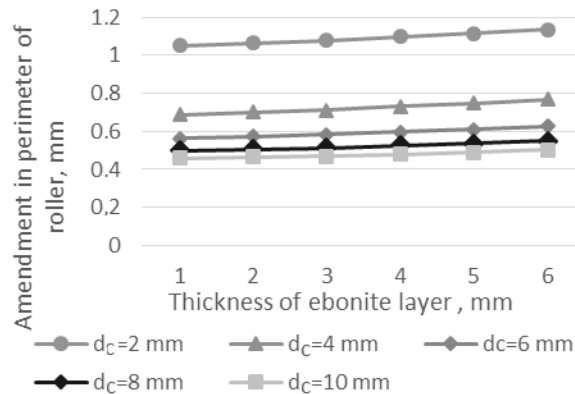


Fig. 12. Parametric analysis

Table 4
Changes in the roller diameters at $D_g = 196$ mm and $D = 180$ mm

Section	Average	Moved to 10 mm	Moved to 30 mm	Moved to 60 mm
Ebonite layer perimeter, mm	615.17	615.17	615.17	615.18
Amendment, mm	0.58	0.58	0.58	0.57

5. CONCLUSION

The applied optimization solution compromise scheme does not deplete the possibilities for subsequent optimization of the many results found, but results from the multicriteria optimization solution can guide the designers to measure the braking performance in a qualitative aspect and support the making of reasoned decisions.

The use of the submodel and the RIMS technique allows the fatigue strength of the welding seam to be tested by a stand used to measure the braking efficiency. The results obtained for a particular geometric configuration, such as boundary conditions and material characteristics, indicate that there is no danger of the structure being destroyed. It is interesting to note the residual stresses of the welding process in the seam and the area around it, and to study the reliability of the computation process at different classes of welding seams.

There is an open question about determining the number of cycles the rubber layer can withstand.

The performed check of the convergence of the results concerning the determination of the stressed and strained state of a calibration double-layer roller shows satisfactory results in terms of their practical appliance.

The performed parametric analysis indicates that the change in the perimeter of the roller is more sensitive to the thickness of a steel layer, instead of an ebonite layer.

The results that are found in this research can be used for qualitative assessment, as well as to select directly the thickness of the ebonite layer in a calibration roller for automotive stands of different purposes.

Acknowledgments

The study was supported by the contract of University of Ruse "Angel Kanchev", No BG05M2OP001-2.009-0011-C01, "Support for the development of human resources for research and innovation at the University of Ruse "Angel Kanchev". The project is funded with support from the Operational Program "Science and Education for Smart Growth 2014–2020" financed by the European Social Fund of the European Union.

References

1. Directive 2009/40/EC of the European Parliament and of the Council of 6 May 2009 on roadworthiness tests for motor vehicles and their trailers.
2. ISO 21069-1:2004. *Road vehicles - Test of braking systems on vehicles with a maximum authorized total mass of over 3.5 t using a roller brake tester - Part 1: Pneumatic braking systems*. International Organization for Standardization.
3. ISO 21995:2008. *Road vehicles - Test of vehicle air braking systems with a permissible mass of over 3.5 t - Acquisition and use of reference values using a roller brake tester*. International Organization for Standardization.
4. Directive 2004/22/EC of the European Parliament and of the Council of 31 March 2004 on measuring instruments.
5. EN 50148:2001. *Електронни таксиметрови апарати*. София: Български институт за стандартизация. [In Bulgarian: *Electronic taximeters*. Sofia: Bulgarian Institute of Standardization].
6. Сестримски, Д. *Диагностика на автомобила*. София: Техника. 1989. 235 p. [In Bulgarian: Sestrimski, D. *Diagnostics of the car*. Sofia: Tehnica].
7. Trzeciak, K. *Diagnostyka samochodow osobowych*. Warszawa: WKL. 2005. 352 p. [In Polish: Trzeciak, K. *Diagnosis of passenger cars*. Warsaw, WKL].
8. Senabre, C. & Velasco, E. & Valero, S. Analysis of the influence on tire pressure and weight on the measure of braking-slide on a brake tester and on flat ground. *Securitas Vialis* 2. 2010. P. 109-116.
9. Senabre, C. & Velasco, E. & Valero, S. Comparative Analysis of Vehicle Brake Data in the Ministry of Transport Test on the Roller Brake Tester and on Flat Ground. *International Journal of Automotive Technology*. 2012. Vol. 13. No. 5. P. 735-742.
10. Pusa, A. Traceability of the calibration of test car for roll brake tester. In: *18th IMEKO TC3 Conference on Force, Mass and Torque*, 2002. P. 298-305.
11. Pusa, A. & Leppälä, H. Investigation of the Measurement Capability of Roll Brake Tester by the Test Trail. In: *XVII IMEKO World Congress*. In: Dubrovnik, Croatia. 2003. P. 362-365.

12. Ramos, D. & Gauchia, A & Boada, B. & Diaz, V. New Procedure to Estimate the Brake Warping in a Roller Tester. *International Journal of Automotive Technology*. 2010. Vol. 11. No. 5. P. 691-699.
13. Ангелов, Б. *Методологически основи на функционално-структурния анализ и проектирането на технически системи*. Русе. 2014. 128 p. [In Bulgarian: Angelov, B. *Methodological foundations of functional-structural analysis and design of technical systems*. Ruse].
14. Стойчев, Ю. & Куюмджиев, Х. & Николов, Й. & Василева, М. *Съпротивление на материалите*. Русе: ВТУ "Ангел Кънчев". 1986. 422 p. [In Bulgarian: Stojchev, Y. & all. *Strength of materials*. Ruse].
15. Иванов, И. *Механика на материалите и конструкциите*. Русе. 2014. 373 p. [In Bulgarian: Ivanov, I. *Mechanics of materials and structures*. Ruse].
16. Salukvadze, M. An Approach to the Solution on the Vector Optimization Problem of Dynamic Systems. *Journal of Theory and Applications*. 1982. Vol. 38. No. 3. P. 409-422.
17. Чешанков, Б. & Витлиемов, В. & Коев, П. Многокритериален параметричен синтез на механични системи: I. Оптимизационен подход. *Механика на машините*. 2000. Vol. 8 (32). No. 4. P. 97-102. [In Bulgarian: Cheshankov, B. & et al. Multi-criterial parametric synthesis of mechanical systems I. Optimization approach. *Mechanics of machines*].
18. Иванов, И. *Компютърно моделиране на непрекъснати среди*. Русе: Русенски университет. 2004. 117 p. [In Bulgarian: Ivanov, I. *Computer modeling of continuum*. Ruse].
19. Radaj, D. *Gestaltung und Berechnung von Schweißkonstruktionen, Ermüdungsfestigkeit*. PhD thesis. Düsseldorf, Germany: DVS. 1985. [In German: Radaj, D. *Design and calculation of welding structures, fatigue strength*. PhD thesis. Dusseldorf, Germany: DVS].
20. Hirai, I. & Wang, B. & Pilkey, W. An efficient zooming method for finite element analysis. *International Journal for Numerical Methods in Engineering*. 1984. Vol. 20. No. 9. P. 1671-1683.
21. Davies, B. The Stress-Strain Relationship in Ebonite. *Transactions of the Institution of the Rubber Industry*. 1933. Vol. 9. No. 2. P. 130-140.
22. Davies, P. & Blackman, B. & Brunner, A. Standard test methods for delamination resistance of composite materials: current status. *Applied Composite Materials*. 1998. Vol. 5. No. 6. P. 345-364.
23. Rizov V. Non-linear delamination fracture analysis by using power-law hardening. *Multidiscipline Modeling in Materials and Structures*. 2016. Vol. 12. No. 1. P. 80-92.
24. Тончев, Й. *MATLAB 7 Част III. Преобразувания. Изчисления. Визуализация*. София: "Техника". 2009. 220 p. [In Bulgarian: Tonchev, I. *MATLAB 7 Part III. Transformations. Calculations. Visualization*. Sofia].
25. ABAQUS. *Analysis User's Manual. ver. 6.12*, USA: Dassault Systemes Simulia Corp.
26. Иванов, Р. & Аврамов, Е. & Русев, Р. Влияние на някои фактори върху контактното петно на пневматична гума. *Научни трудове на Русенски университет*. 2011. Vol. 50. Ser. 4. P. 65-70. [In Bulgarian: Ivanov, R. & all. Influence of some factors on the contact spot of the tire. *Proceedings -University of Ruse*].
27. Желев, А. & Костадинов, Й. *Заварени конструкции. Том II. Якостни оценки*. София: Държавно издателство „Техника“. 1984. 203 p. [In Bulgarian: Gelev, A. & all. *Welded structures II. Strength assessments*. Sofia].